

AGILE OBSERVATIONS OF THE “SOFT” GAMMA-RAY PULSAR PSR B1509–58

M. PILIA^{1,2}, A. PELLIZZONI², A. TROIS³, F. VERRECCHIA⁴, P. ESPOSITO^{2,5}, P. WELTEVREDE^{6,7}, S. JOHNSTON⁶, M. BURGAY², A. POSSENTI², E. DEL MONTE³, F. FUSCHINO⁸, P. SANTOLAMAZZA⁴, A. CHEN^{9,10}, A. GIULIANI⁹, P. CARAVEO⁹, S. MEREGHETTI⁹, M. TAVANI^{3,11}, A. ARGAN³, E. COSTA³, N. D’AMICO², A. DE LUCA^{5,9,12}, Y. EVANGELISTA³, M. FEROCI³, F. LONGO¹³, M. MARISALDI⁸, G. BARBIELLINI¹³, A. BULGARELLI⁸, P. W. CATTANEO⁵, V. COCCO³, F. D’AMMANDO^{3,11,14}, G. DE PARIS³, G. DI COCCO⁸, I. DONNARUMMA³, M. FIORINI⁹, T. FROYSLAND^{10,11}, M. GALLI¹⁵, F. GIANOTTI⁸, C. LABANTI⁸, I. LAPSHOV³, F. LAZZAROTTO³, P. LIPARI¹⁶, A. MORSELLI¹⁷, L. PACCIANI³, F. PEROTTI⁹, G. PIANO^{3,11}, P. PICOZZA¹⁷, M. PRESTI¹, G. PUCCELLA¹⁸, M. RAPISARDA¹⁸, A. RAPPOLDI⁵, S. SABATINI^{3,16}, P. SOFFITTA³, M. TRIFOGLIO⁸, E. VALLAZZA¹³, S. VERCELLONE¹⁴, V. VITTORINI¹¹, A. ZAMBRA⁹, D. ZANELLO¹⁶, C. PITTORI⁴, F. LUCARELLI⁴, P. GIOMMI⁴, L. SALOTTI¹⁹, AND G. F. BIGNAMI¹²

¹ Dipartimento di Fisica, Università dell’Insubria, Via Valleggio 11, I-22100 Como, Italy; mpilia@ca.astro.it

² INAF-Osservatorio Astronomico di Cagliari, località Poggio dei Pini, strada 54, I-09012 Capoterra, Italy

³ INAF/IASF-Roma, Via del Fosso del Cavaliere 100, I-00133 Roma, Italy

⁴ ASI-ASDC, Via G. Galilei, I-00044 Frascati, Roma, Italy

⁵ INFN-Pavia, Via Bassi 6, I-27100 Pavia, Italy

⁶ Australia Telescope National Facility, CSIRO, P.O. Box 76, Epping NSW 1710, Australia

⁷ Jodrell Bank Centre for Astrophysics, The Alan Turing Building, School of Physics and Astronomy, The University of Manchester, Oxford Road, Manchester, M13 9PL, UK

⁸ INAF/IASF-Bologna, Via Gobetti 101, I-40129 Bologna, Italy

⁹ INAF/IASF Milano, Via E. Bassini 15, I-20133 Milano, Italy

¹⁰ CIFS-Torino, Viale Settimio Severo 3, I-10133, Torino, Italy

¹¹ Dipartimento di Fisica, Università “Tor Vergata,” Via della Ricerca Scientifica 1, I-00133 Roma, Italy

¹² Istituto Universitario di Studi Superiori, V.le Lungo Ticino Sforza 56, 27100 Pavia, Italy

¹³ Dipartimento di Fisica, Università di Trieste and INFN-Trieste, Via Valerio 2, I-34127 Trieste, Italy

¹⁴ INAF/IASF Palermo via U. La Malfa 153, I-90146, Palermo, Italy

¹⁵ ENEA-Bologna, Via Biancamano 2521, I-40059 Medicina, Bologna, Italy

¹⁶ INFN-Roma “La Sapienza,” Piazzale A. Moro 2, I-00185 Roma, Italy

¹⁷ INFN-Roma “Tor Vergata,” Via della Ricerca Scientifica 1, I-00133 Roma, Italy

¹⁸ ENEA-Roma, Via E. Fermi 45, I-00044 Frascati, Roma, Italy

¹⁹ ASI, Viale Liegi 26, I-00198 Roma, Italy

Received 2010 March 30; accepted 2010 August 24; published 2010 October 13

ABSTRACT

We present the results of new *AGILE* observations of PSR B1509–58 performed over a period of ~ 2.5 years following the detection obtained with a subset of the present data. The modulation significance of the light curve above 30 MeV is at a 5σ confidence level and the light curve is similar to those found earlier by *COMPTEL* up to 30 MeV: a broad asymmetric first peak reaching its maximum 0.39 ± 0.02 cycles after the radio peak plus a second peak at 0.94 ± 0.03 . The gamma-ray spectral energy distribution of the pulsed flux detected by *COMPTEL* and *AGILE* is well described by a power law (photon index $\alpha = 1.87 \pm 0.09$) with a remarkable cutoff at $E_c = 81 \pm 20$ MeV, representing the softest spectrum observed among gamma-ray pulsars so far. The pulsar luminosity at $E > 1$ MeV is $L_\gamma = 4.2^{+0.5}_{-0.2} \times 10^{35}$ erg s⁻¹, assuming a distance of 5.2 kpc, which implies a spin-down conversion efficiency to gamma rays of ~ 0.03 . The unusual soft break in the spectrum of PSR B1509–58 has been interpreted in the framework of polar cap models as a signature of the exotic photon-splitting process in the strong magnetic field of this pulsar. In this interpretation, our spectrum constrains the magnetic altitude of the emission point(s) at 3 km above the neutron star surface, implying that the attenuation may not be as strong as formerly suggested because pair production can substitute photon splitting into regions of the magnetosphere where the magnetic field becomes too low to sustain photon splitting. In the case of an outer-gap scenario or the two-pole caustic model, better constraints on the geometry of the emission would be needed from the radio band in order to establish whether the conditions required by the models to reproduce *AGILE* light curves and spectra match the polarization measurements.

Key words: gamma rays: stars – pulsars: general – pulsars: individual (PSR J1513–5908 (B1509–58)) – stars: neutron

Online-only material: color figure

1. INTRODUCTION

PSR B1509–58 (J1513–5908) was discovered as an X-ray pulsar with the *Einstein* satellite during an observation of the supernova remnant (SNR) MSH 15–52 (Seward & Harnden 1982). The source was soon also detected at radio frequencies by Manchester et al. (1982), with a derived distance supporting the association with the SNR ($d \sim 5.2$ kpc, as calculated from H I measurements from Gaensler et al. (1999) and in agreement

with the most recent distance derived using the dispersion measure²⁰). With a period $P \simeq 150$ ms and a period derivative $\dot{P} \simeq 1.53 \times 10^{-12}$ s⁻¹, assuming the standard dipole vacuum model, the estimated spin-down age for this pulsar is 1570 years (among the shortest for radio pulsars) and its inferred surface

²⁰ See the ATNF Pulsar Catalogue (<http://www.atnf.csiro.au/research/pulsar/psrcat/>) for the updated distance measurement derived from the dispersion measure.

magnetic field is one of the highest observed for an ordinary radio pulsar: $B = 3.1 \times 10^{13}$ G, as calculated at the pole.²¹ Its rotational energy loss rate is $\dot{E} = 1.8 \times 10^{37}$ erg s⁻¹.

PSR B1509–58 and its nebula have been extensively observed in the X-ray energies since the 1980s with the *Einstein* and *EXOSAT* satellites. The detection of pulsed emission in the hard X-rays dates back to the early 1990s (Kawai et al. 1991) with *Ginga* in the 2–60 keV energy range. During a 20 yr long radio monitoring (Livingstone et al. 2005), PSR B1509–58 has not shown any glitch activity, at variance with the general behavior of young radio pulsars, which usually show some glitch activity. The analysis of Livingstone et al. (2005), using radio and X-rays (collected with *RossixTE*), yielded a very accurate measurement of the braking index of $n = 2.839 \pm 0.003$, close to the canonical value $n = 3$ for braking by magnetic dipole radiation in vacuum alone. Observations with the *ROSAT* (Trussoni et al. 1996), *ASCA* (Tamura et al. 1996), and *BeppoSAX* (Mineo et al. 2001) satellites were performed in the 1990s, characterizing the spectrum of the pulsed emission and the morphology of the remnant as possibly due to the presence of several components, interacting via collimated outflows from the pulsar. The nebula has been extensively observed with the *Chandra* satellite (Gaensler et al. 2002), and its emission has been found up to the TeV energies, with *CANGAROO* first (Sako et al. 2000) and more recently by *H.E.S.S.* (Aharonian et al. 2005).

The young age and the high rotational energy loss rate made this pulsar a promising target for the first generation of gamma-ray satellites. In fact, the instruments on the *Compton Gamma-Ray Observatory* (*CGRO*) observed its pulsation at low gamma-ray energies up to $E \sim 700$ keV with *BATSE* (Wilson et al. 1993) and *OSSE* (Ulmer et al. 1993; Matz et al. 1994), and in the 0.75–30 MeV band with *COMPTEL* (Kuiper et al. 1999), but it was not detected with high significance by the *Energetic Gamma-Ray Experiment Telescope* (*EGRET*), the instrument operating at the energies from 30 MeV to 30 GeV. This was remarkable, since all other known gamma-ray pulsars show spectral turnovers well above 100 MeV (Thompson 2004). Harding et al. (1997) suggested that the break in the spectrum could be interpreted as due to inhibition of the pair production caused by the photon-splitting phenomenon (Adler et al. 1970). The photon splitting appears, in the frame of the polar cap models, in relation with a very high magnetic field. An alternative explanation is proposed by Zhang & Cheng (2000) using a three-dimensional outer gap model. They propose that the gamma-ray emission is produced by synchrotron-self-Compton radiation above the outer gap.

Ten years after the *CGRO*, observation in the gamma-ray band is again possible with the advent of two high-energy missions: the *Astro-rivelatore Gamma a Immagini LEggero* (*AGILE*) and *Fermi* satellites. With its large field of view (~ 2.5 sr) and its $\lesssim 1$ μ s time tagging capability (Tavani et al. 2009; with 200 μ s absolute timing accuracy; see Pellizzoni et al. 2009b), *AGILE* is very well suited for the observation of pulsars between 30 MeV and a few GeV with its *Gamma-Ray Imaging Detector* (*GRID*). In particular, despite its lower sensitivity in the GeV band, the *GRID* on board *AGILE* has an effective area below 100 MeV (~ 200 cm² at 50 MeV) comparable with that of *Fermi*. *AGILE* obtained the first detection of PSR B1509–58 in the *EGRET* band (Pellizzoni et al. 2009a) confirming the occurrence of a spectral break, although no precise flux measurements were possible due to low count statistics.

Recently, *Fermi* also reported its detection of PSR B1509–58 (Abdo et al. 2010a). In this paper, we present the results of a ~ 2.5 year monitoring campaign of PSR B1509–58 with *AGILE* that improved counts statistics, and therefore light-curve characterization, with respect to earlier *AGILE* observations. With these observations the spectral energy distribution (SED) at energies $E < 300$ MeV, where the remarkable spectral turnover is observed, can be assessed.

2. *AGILE* OBSERVATIONS, DATA ANALYSIS, AND RESULTS

PSR B1509–58 is within the same region of the sky as the Vela pulsar, an area to which *AGILE* devoted a large amount of observing time (for details on *AGILE* observing strategy, timing calibration, and gamma-ray pulsars analysis; see Pellizzoni et al. 2009a, 2009b). Gamma-ray photons for this pulsar were collected and analyzed starting in 2007 July, up to late 2009 October when *AGILE* started observing in spinning mode due to reaction wheel failure.²² The large *AGILE* effective area and long observing time (~ 260 days on target) provide a total exposure of 3.8×10^9 cm² s ($E > 100$ MeV) during this 2.5 yr period which gives our observations a good photon harvest from this pulsar.

2.1. Timing Analysis

Simultaneous radio observations of PSR B1509–58 with the 64 m Parkes radio telescope in Australia are ongoing since the epoch of *AGILE*'s launch (MJD 54,220; 2007 April 30), as part of a timing project for the gamma-ray satellites (Weltevrede et al. 2010b), and cover all of *AGILE*'s observations. A total of 47 pulsar time of arrivals (ToAs) were collected between 2007 April (MJD 54,220) and 2010 February (MJD 55,233), leading to an rms of the residuals of 900 μ s, showing the goodness of the timing model that allowed accurate pulse phase tagging of the gamma-ray photons. No glitch was detected in the radio analysis. Strong timing noise was present, as expected from a young pulsar, and it was accounted for using the fitwaves technique developed in the framework of the TEMPO2 radio pulsar timing software (Hobbs et al. 2004, 2006). Using the radio ephemeris provided by the Parkes telescope, we performed the folding of the gamma-ray light curve including the wave terms (see Pellizzoni et al. 2009b). An optimized analysis followed, aimed at cross-checking and maximization of the significance of the detection, including an energy-dependent event extraction angle around the source position based on the instrument point-spread function (PSF). Only high confidence gamma-ray photons (G) were used for the timing analysis of this pulsar. The chi-squared (χ^2) test applied to the 10 bin light curve at $E > 30$ MeV gave a detection significance of $\sigma = 4.8$. The unbinned Z_n^2 -test applied to the photons' arrival times gave a significance of $\sigma = 5.0$ with $n = 2$ harmonics. The difference between the radio and gamma-ray ephemerides was $\Delta P_{\text{radio},\gamma} \lesssim 10^{-9}$ s, well within the error in the parameters, showing perfect agreement among radio and gamma-ray ephemerides as expected, further supporting our detection and *AGILE* timing calibration.

We observed PSR B1509–58 in three energy bands. We obtained 1210 ± 400 pulsed counts ($\sim 5\%$ of the total source, diffuse gamma-ray emission, and residual particle background

²¹ The magnetic field strength at the pole is twice the value quoted in the ATNF Pulsar Catalogue.

²² This failure is not affecting *AGILE/GRID* sensitivity and pulsar observations, although the new spinning mode required calibration revisions that are still ongoing.

counts) at energies $30 < E < 100$ MeV and 820 ± 360 pulsed counts ($\sim 7\%$ of the total counts) at energies $100 < E < 500$ MeV. The pulsed flux was computed considering all the counts above the minimum of the light curve (see Pellizzoni et al. 2009b). We did not detect pulsed emission at a significance $\sigma \geq 2$ for $E > 500$ MeV and thus we can only give an upper limit at 1σ of < 270 pulsed counts. This is consistent with the fact that Abdo et al. (2010a) report only a 1.4σ detection at $0.3 < E < 1$ GeV with the *Fermi* data.

The gamma-ray light curves of PSR B1509–58 for different energy bands are shown in Figure 1. The *AGILE* light curve above 30 MeV shows two peaks at phases $\phi_1 = 0.39 \pm 0.02$ and $\phi_2 = 0.94 \pm 0.03$ with respect to the single radio peak, here put at phase 0, as obtained from the Parkes ephemeris. The peak positions and widths in terms of phase are calculated using a Gaussian fit, yielding an FWHM of 0.29(6) for the first peak and of 0.13(7) for the second peak, where we quote in parentheses (here and throughout the paper) the 1σ error on the last digit. The errors considered are statistical, as the systematic errors do not affect the measurements of the pulsed counts. The first peak is coincident in phase with the X-ray single broad peak and with the *COMPTEL* peak (see Kuiper et al. 1999, and references therein). In its highest energy band (10–30 MeV) *COMPTEL* showed the hint of a second peak (even though the modulation had low significance, 2.1σ), which is also visible in the light curve derived from *EGRET* observations (30–100 MeV), despite the fact that *EGRET* did not have a significant detection of the pulsar above 100 MeV (Fierro 1995). This second peak is coincident in phase with *AGILE*'s second peak (Figure 1) in its lower energy band, while it appears slightly shifted at energies above 100 MeV. A possible explanation for this shift is discussed in Section 3. *AGILE* thus confirms the previously marginal detection of a second peak, statistically significant at 5σ , calculated using a chisquared statistics test.

2.2. Spectral Analysis and Spectral Energy Distribution

Based on our exposure, calculated by the *GRID* scientific analysis task AG_ExmapGen, we derived the gamma-ray flux from the number of pulsed counts. This method, though typically giving higher statistical errors than the likelihood analysis, is more accurate and sensitive to evaluate the flux of this pulsar, given its soft spectrum (and the correspondingly large PSF) and the contribution from other nearby and brighter sources and possibly from the pulsar wind nebula (PWN), that all affect the spatial analysis. Using this method, the problem of modeling the background is dealt with by discarding the counts below the pulsed threshold, so that the observed pulsed counts belong to the pulsar. All the other sources of systematical errors related to the effective area, *AGILE*'s PSF and energy dispersion, contribute to $< 10\%$, so that they are much lower than the statistical errors and they are not quoted in the flux measurements. We divided *AGILE* bandwidth into three energy intervals: 30–100 MeV, 100–500 MeV, and above 500 MeV. The pulsed fluxes thus obtained were $F_\gamma = 10(3) \times 10^{-7}$ ph cm $^{-2}$ s $^{-1}$ in the 30–100 MeV band, $F_\gamma = 1.8(8) \times 10^{-7}$ ph cm $^{-2}$ s $^{-1}$ in the 100–500 MeV band, and a 1σ upper limit $F_\gamma < 8 \times 10^{-8}$ ph cm $^{-2}$ s $^{-1}$ for $E > 500$ MeV. Finally, from the total number of pulsed counts we obtained a pulsed flux at $E > 30$ MeV $F_\gamma = 12(2) \times 10^{-7}$ ph cm $^{-2}$ s $^{-1}$ for $E > 30$ MeV.

Figure 2 shows the SED of PSR B1509–58 based on *AGILE*'s and *COMPTEL*'s observed fluxes. *Fermi* upper limits are also shown, which are consistent with our measurements at a 2σ confidence level. *COMPTEL* observed this pulsar in three energy

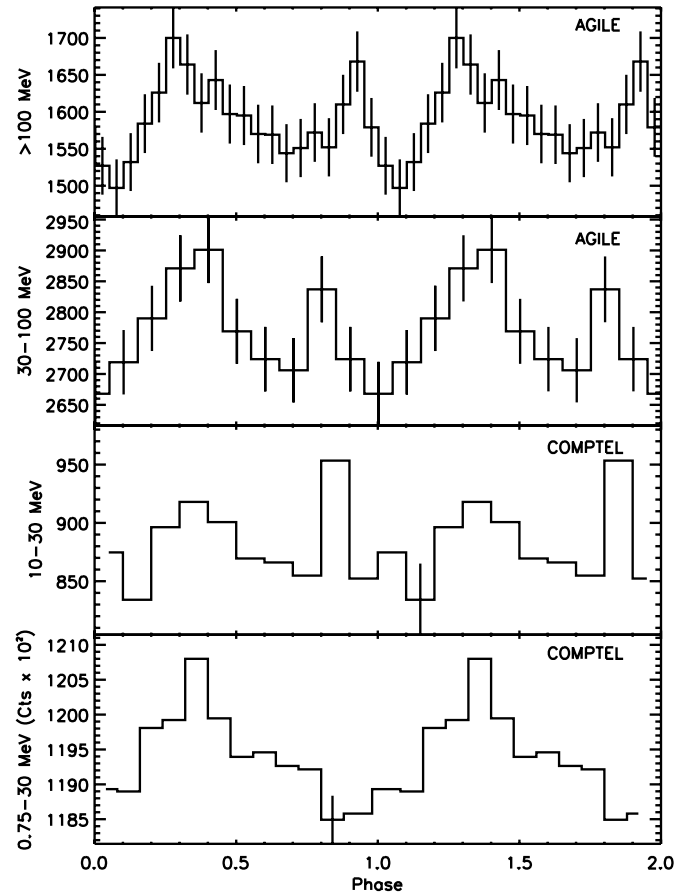


Figure 1. Phase-aligned gamma-ray light curves of PSR B1509–58. Radio main peak is at phase 0. The start of the y-axis coincides with the minimum of the pulsed fraction and, consequently, with the background level. From top to bottom: *AGILE* high-energy band (> 100 MeV), 20 bins, 7.5 ms resolution; *AGILE* “soft” energy band (< 100 MeV), 10 bins, 15 ms resolution; *COMPTEL* high-energy band (10–30 MeV) and *COMPTEL* whole bandwidth (0.75–30 MeV; from Kuiper et al. 1999).

bands: 0.75–3 MeV, 3–10 MeV, 10–30 MeV, suggesting a spectral break between 10 MeV and 30 MeV. *AGILE* pulsed flux confirms the presence of a soft spectral break. As shown in Figure 2, we modeled the observed *COMPTEL* and *AGILE* fluxes with a power law plus cutoff fit using the Minuit minimization package (James & Roos 1975): $F(E) = k \times E^{-\alpha} \exp[-(E/E_c)^\beta]$, with three free parameters: the normalization k , the spectral index α , the cutoff energy E_c and allowing β to assume values of 1 and 2 (indicating either an exponential or a superexponential cutoff). No acceptable χ^2 values were obtained for a superexponential cutoff, the presence of which can be excluded at a 3.5σ confidence level, while for an exponential cutoff we found $\chi^2_\nu = 3.2$ for $\nu = 2$ degrees of freedom, corresponding to a null hypothesis probability of 0.05. The best values thus obtained for the parameters of the fit were $k = 1.0(2) \times 10^{-4}$ s $^{-1}$ cm $^{-2}$, $\alpha = 1.87(9)$, and $E_c = 81(20)$ MeV.

We performed an analysis of the ratio between the two peak heights. The second peak appears in the *COMPTEL* band 10–30 MeV and is observed with *AGILE* up to $E \lesssim 500$ MeV: it is harder than the first peak in the *COMPTEL* energy band, and it is present at all energies in the *AGILE* energy band, so that it might possibly be harder even at *AGILE*'s energies but the low statistics at high energies do not allow us to discriminate.

As a consistency check for the pulsed fluxes reported above, a maximum likelihood analysis in a region of 10° around the

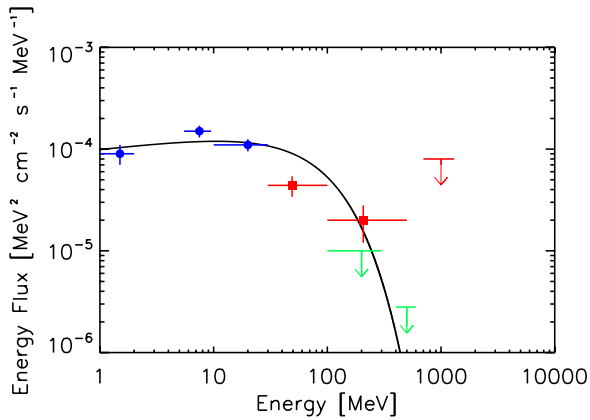


Figure 2. SED of PSR B1509–58 (solid line) obtained from a fit of pulsed fluxes from soft to hard gamma rays. The three round points represent *COMPTEL* observations (Kuiper et al. 1999). The two square points represent *AGILE* pulsed flux in two bands ($30 < E < 100$ MeV and $100 < E < 500$ MeV). The red horizontal bar and arrow emerging from it represent the *AGILE* upper limit above 500 MeV. The two green arrows represent *Fermi* upper limits (Abdo et al. 2010a).

(A color version of this figure is available in the online journal.)

source position was performed to assess possible unpulsed contribution from the PWN,²³ although no detection was reported in the First Catalog of High-Confidence Gamma-ray Sources detected by the *AGILE* satellite (Pittori et al. 2009). The likelihood analysis (see Mattox et al. (1996), and for *AGILE* in particular, details will be provided in A. Chen et al. 2010, in preparation) took into account the numerous sources present in this crowded region (including the extremely bright nearby gamma-ray pulsar J1509–5850; Weltevrede et al. 2010a). The upper limit found in the *AGILE* energy range by likelihood analysis ($F_\gamma < 40 \times 10^{-8}$ ph cm⁻² s⁻¹ above 100 MeV) is above the corresponding pulsed flux above 100 MeV ($F_\gamma = 21(6) \times 10^{-8}$ ph cm⁻² s⁻¹). This is compatible with the fact that the timing analysis is expected to have for this target a better sensitivity (with respect to the likelihood analysis). It is worth noting that PSR B1509–58 is also not detected by likelihood analysis by *Fermi* (Abdo et al. 2010a) apart from the > 1 GeV energy band where the emission could be related to the PWN seen by *H.E.S.S.* (Aharonian et al. 2005).

3. DISCUSSION

Pulsar magnetosphere models are usually divided into two categories, depending on the sites for the high-energy emission. In polar cap models (Daugherty & Harding 1996), the emission comes from the regions near the neutron star surface, while outer gap models (Cheng et al. 1986; Romani 1996) predict that the emission will originate in the regions close to the light cylinder. Alternative models predict an emission zone encompassing the whole magnetosphere, which departs from the external rim of the polar cap region: these are the slot gap models (Muslimov & Harding 2003); others predict emission from alternative regions in the outer magnetosphere, the annular gap models (Du et al. 2010, and references therein). Different models predict different spectral and geometrical properties. The bulk of the spin-powered pulsar flux is usually emitted in the MeV–GeV energy band with spectral breaks at $\lesssim 10$ GeV (see Abdo et al. 2010b or, e.g., Aliu et al. 2008). PSR B1509–58

has the softest spectrum observed among gamma-ray pulsars, with a sub-GeV cutoff at $E = 0.08(2)$ GeV. The second softest spectrum and lowest energy cutoff (0.7(5) GeV) is that of PSR B0656+14, recently observed by *Fermi* (Weltevrede et al. 2010a). The observed light curve of PSR B1509–58 shows two peaks lagging the radio peak by, respectively, $\phi_1 = 0.39 \pm 0.02$ and $\phi_2 = 0.94 \pm 0.03$. In the following, we discuss how the new *AGILE* observations can constrain the models for emission from the pulsar magnetosphere.

When PSR B1509–58 was detected in soft gamma rays but not significantly at $E > 30$ MeV, it was proposed that the mechanism responsible for this low-energy spectral break might be photon splitting (Harding et al. 1997). Photon splitting (Adler et al. 1970) is an exotic third-order quantum electrodynamics (QED) process expected when the magnetic field approaches or exceeds the *critical* value defined as $B_{\text{cr}} = m_e^2 c^3 / (e\hbar) = 4.413 \times 10^{13}$ G, above which quantum effects become relevant. Most current theories for the generation of coherent radio emission in pulsar magnetospheres require formation of an electron–positron pair plasma developing via electromagnetic cascades. In very high magnetic fields, the formation of pair cascades can be altered by the process of photon splitting: $\gamma \rightarrow \gamma\gamma$, which will operate as an attenuation mechanism in the high-field regions near pulsar polar caps. Since it has no energy threshold, photon splitting can attenuate photons below the threshold for pair production, thus determining a spectral cutoff at lower energies. This process cannot operate in the low fields of outer gap models because it only has appreciable reaction rates when the magnetic field is at least a significant fraction of the quantum critical field B_{cr} (the attenuation coefficient T_{sp} scaling as $T_{\text{sp}} \propto (B/B_{\text{cr}})^6 = B'^6$) and magnetic fields strong enough are not present in the outer magnetosphere as $B \sim r^{-3}$.

In the case of PSR B1509–58, a polar cap model with photon splitting would be able to explain the soft gamma-ray emission and the low-energy spectral cutoff, now quantified by *AGILE* observations. Since the mechanism of photon splitting is, as stated, strongly dependent on the magnetic field strength, if the field strength at the emitting region is $B' \gtrsim 0.3$ (i.e., at heights below 1.3 neutron star radii, R_{NS}), photon splitting is the dominant means of attenuation that inhibits efficient pair cascade production (Harding et al. 1997) and then gamma-ray emission. Based on the observed cutoffs, which are related to the photons' saturation escape energy, we can derive constraints on the magnetic field strength at emission, in the framework of photon splitting:

$$\epsilon_{\text{esc}}^{\text{sat}} \simeq 0.077(B' \sin \theta_{kB,0})^{-6/5}, \quad (1)$$

where $\epsilon_{\text{esc}}^{\text{sat}}$ is the photon saturation escape energy and $\theta_{kB,0}$ is the angle between the photon momentum and the magnetic field vectors at the surface and is here assumed to be very small: $\theta_{kB,0} \lesssim 0.57$ (see Harding et al. 1997). Using the observed energy cutoff ($\epsilon_{\text{esc}}^{\text{sat}} \simeq E = 80$ MeV), we find that $B' \gtrsim 0.3$, which implies an emission altitude $\lesssim 1.3 R_{\text{NS}}$, which is the height where pair production could also possibly ensue. This altitude of emission agrees with the polar cap models (see, e.g., Daugherty & Harding 1996). A smaller energy cutoff, as in Harding et al. (1997), would have implied even lower emission altitude and a sharper break, possibly caused by the total absence of pair production. It is apparent that small differences in the emission position will cause strong differences in spectral shape. This is possibly the reason for the different emission properties of the two peaks as observed in the total (*AGILE* plus *COMPTEL*)

²³ See, e.g., Pellizzoni et al. (2010) as an example of study of gamma-ray PWN with *AGILE*.

gamma-ray energy band. Also, a trend can be observed, from lower to higher energies (see the X-ray light curve for the trend in the first peak, as in Figure 3 of Kuiper et al. 1999), of the peaks slightly drifting away from the radio peak. This we assume to be another signature of the fact that small variations in emission height can be responsible for sensible changes in the light curves in such a high magnetic field. The scenario proposed by Harding et al. (1997) is strengthened by its prediction that PSR B0656+14 should have a cutoff with an intermediate value between PSR B1509–58 and the other gamma-ray pulsars. The main reason for the parallel between the two pulsars at the time was the fact that they had, respectively, the highest and second highest inferred magnetic fields. At present, however, there are a handful of gamma-ray pulsars with higher magnetic field than PSR B0656+14 in the *Fermi* First Year Pulsar Catalog (Abdo et al. 2010b) which do not show a low-energy cutoff. Nonetheless, both PSR B1509–58 (see Kuiper et al. 1999; Crawford et al. 2001) and PSR B0656+14 (De Luca et al. 2005; Weltevrede et al. 2010a) show evidence of being aligned rotators, which could imply polar cap emission, as is also hinted by Bai & Spitkovsky (2010).

A soft cutoff (below 1 GeV) is in principle possible for polar cap scenarios even without invoking photon-splitting attenuation. In polar cap models, the strong magnetic field permits one-photon pair creation that attenuates super-GeV photons in Crab-like (e.g., PSR B1509–58 based on the parameter B/P^2) and Vela-like pulsars (e.g., PSR B0656+14), whereas pair creation in outer gap models is mediated through the two-photon process involving surface thermal X-rays as targets. According to the calculations of Daugherty & Harding (1996), emission from the regions close to the polar caps is possible when $\alpha \sim \theta_b$, where α is the angle between the rotational and the magnetic axes and θ_b is the half-angle of the gamma beam emerging from the polar cap. Furthermore, with emission from the polar caps or some (≥ 2) polar cap radii, the pulse profile at high energies can have either one (as in the case of PSR B0656+14) or two peaks, with a peak-to-peak phase separation as large as 0.4–0.5 (albeit slightly smaller than what is observed for PSR B1509–58 at the highest energies).

The polar cap model as an emission mechanism is nowadays debated. On one hand, theoretical objections arise from the fact that the angular momentum is not conserved in polar cap emission (see Cohen & Treves 1972; Holloway 1977; A. Treves et al. 2010, in preparation). At the same time, mounting evidence of a preferential explanation of the observed gamma-ray light curves with high altitude cascades is also coming from the recent results by the *Fermi* satellite (see, e.g., Abdo et al. 2010b). In the case of PSR B1509–58, the derived gamma-ray luminosity from the flux at $E > 1$ MeV, considering a 1 sr beam sweep is $L_\gamma = 4.2_{-0.2}^{+0.5} d_{5.2}^2 \times 10^{35}$ erg s $^{-1}$, where $d_{5.2}$ indicates the distance in units of 5.2 kpc. While traditionally the beaming fraction (f_Ω) was considered to be the equivalent of a 1 sr sweep, nowadays (see, e.g., Watters et al. 2009) the tendency is to consider a larger beaming fraction ($f_\Omega \approx 1$), close to a 4π sr beam. Using $f_\Omega = 1$ in our calculations, we would have obtained $L_\gamma = 5.8_{-0.8}^{+0.1} d_{5.2}^2 \times 10^{36}$ erg s $^{-1}$. Thus, the maximum conversion efficiency of the rotational energy loss ($\dot{E} \approx 1.8 \times 10^{37}$ erg s $^{-1}$, see Section 1) into gamma-ray luminosity is 0.3. Our result is not easily comparable with the typical gamma-ray luminosities above 100 MeV, because for PSR B1509–58 this energy band is beyond the spectral break. Using *AGILE* data alone we obtained a luminosity above 30 MeV, $L_\gamma = 5.2(6) d_{5.2}^2 \times 10^{35}$ erg s $^{-1}$, again for a 1 sr beam. If the gamma-ray luminosity cannot

account for a large fraction of the rotational energy loss, then the angular momentum conservation objection from Cohen & Treves (1972) becomes less cogent for this pulsar, exactly as it happens for the radio emission. For PSR B0656+14, no outer magnetosphere emission model seemed to satisfy the observed features and a lower magnetosphere model, with an aligned geometry between the rotational and magnetic axes, has been proposed and seems plausible from polarization studies. Its efficiency in the conversion of the rotational energy loss into gamma-ray luminosity is one of the lowest observed for the gamma-ray pulsars (see Pellizzoni et al. 2009a; Abdo et al. 2010b), $\eta = 0.01$, not violating the constraints imposed by the conservation of angular momentum.

Alternatively, if such an efficiency as that of PSR B1509–58 were incompatible with this conservation law, an interpretation of PSR B1509–58 emission should be sought in the frame of the three-dimensional outer magnetosphere gap model, as was done by Zhang & Cheng (2000). According to their model, hard X-rays and low-energy gamma rays have the same origin; they are produced by synchrotron-self-Compton radiation of secondary electron–positron pairs of the outer gap. Therefore, as observed, the phase offset of hard X-rays and low-energy gamma rays with respect to the radio pulse is the same, with the possibility of a small lag due to the thickness of the emission region. According to Zhang & Cheng (2000) estimates, a magnetic inclination angle $\alpha \approx 60^\circ$ and a viewing angle $\zeta \approx 75^\circ$ are required to reproduce the observed light curve. Similarly, for PSR B0656+14, Weltevrede et al. (2010a) argue that large α and ζ angles are required to reproduce the observed light curve in the framework of outer gap models. Finally, using the simulations of Watters et al. (2009), who produced a map of pulse profiles for different combinations of angles α and ζ in the different emission models, the observed light curve from *AGILE* is best reproduced if $\alpha \approx 35^\circ$ and $\zeta \approx 90^\circ$, in the framework of the two-pole caustic model (Dyks & Rudak 2003).

Since the parameters used for the application of the outer gap model to PSR B1509–58 were based on its former observations by *COMPTEL*, the *AGILE* spectrum does not precisely fit the spectrum predicted by the model of Zhang & Cheng (2000). Furthermore, the values of α and ζ required by this model are not in good agreement with the corresponding values obtained with radio measurements. In fact, Crawford et al. (2001) observe that α must be $< 60^\circ$ at the 3σ confidence level. The prediction obtained by the simulations of Watters et al. (2009) for slot gap emission is in better agreement with the radio polarization observations than that predicted in the outer gap framework. In fact, in the framework of the rotating vector model (RVM; see, e.g., Lorimer & Kramer 2004, and references therein), Crawford et al. (2001) also propose that, if the restriction is imposed that $\zeta > 70^\circ$ (Melatos 1997), then $\alpha > 30^\circ$ at the 3σ level. For these values, however, the Melatos model for the spin down of an oblique rotator predicts a braking index $n > 2.86$, slightly inconsistent with the observed value ($n = 2.839(3)$, see Section 1). Also, in the case of PSR B0656+14, Weltevrede et al. (2010a) conclude that the large values of α and ζ are somewhat at odds with the constraints from the modeling of the radio data and the thermal X-rays which seem to imply a more aligned geometry. Improved radio polarization measurements would help placing better constraints on the pulsar geometry and therefore on the possibility of a gap in the extended or outer magnetosphere, but the quality of the polarization measurements from Crawford et al. (2001) is already excellent, the problem being that PSR B1509–58, like most

pulsars, only shows emission over a limited pulse phase range and therefore the RVM models are highly degenerate. At present, the geometry privileged by the state-of-the-art measurements is best compatible with polar cap models. Higher statistics in the number of observed gamma-ray pulsars could help characterize a class of “outliers” having gamma-ray emission from the polar caps, which potentially constitute a privileged target for *AGILE*.

4. CONCLUSIONS

In this paper, we present the result of a 2.5 yr long observation campaign of PSR B1509–58 with *AGILE*. With respect to our previous work (Pellizzoni et al. 2009a), the increased statistics allowed us to perform an improved light-curve analysis and to better constrain the soft spectral cutoff observed for this pulsar.

1. Using the Parkes radio ephemeris, *AGILE* firmly confirmed the detection of gamma-ray pulsation with good significance ($\sim 5\sigma$) from PSR B1509–58.
2. The observed light curve shows two peaks which lag the radio peak of, respectively, 0.39 ± 0.02 and 0.94 ± 0.03 cycles, as obtained from a Gaussian fit of the peaks. PSR B1509–58 presents a single-peaked profile up to energies $E > 10$ MeV where *COMPTEL* detected an additional peak with lower significance. *AGILE* confirmed the existence of this second harder peak in the 30–500 MeV energy band.
3. The detection of pulsed emission by *AGILE* at $E > 30$ MeV, confirming the presence of a soft spectral break, moves the cutoff slightly up, to $E \approx 80$ MeV, in agreement with the previous estimates of a cutoff at energies below 100 MeV.

Our observations are compatible with emission from the polar cap regions powered by photon-splitting cascades. This interpretation could represent a physical measurement related to the QED photon-splitting process. The fact that polar cap emission at high energies appears rare might be explained by the requirement that a number of conditions concur to have low magnetosphere emission: an aligned geometry and a high magnetic field, without conflicting with the conservation laws. With the *AGILE* capability of observing with good sensitivity at $E > 30$ MeV, it will be interesting to investigate the highly magnetized pulsar population as a possible contributor to a new class of “soft” gamma-ray pulsars. Alternative emission models rely on better knowledge of the geometry of PSR B1509–58.

The authors thank the anonymous referee for the constructive comments. M.P. thanks Aldo Treves for useful discussion and comments and acknowledges the University of Insubria-Como for financial support. The *AGILE* Mission is funded by the Italian Space Agency (ASI) and programmatic participation by the Italian Institute of Astrophysics (INAF) and the Italian Institute of Nuclear Physics (INFN). The Parkes radio telescope is part of the Australia Telescope, funded by the Commonwealth Government for operation as a National Facility managed by CSIRO.

REFERENCES

- Abdo, A. A., et al. 2010a, *ApJ*, 714, 927
 Abdo, A. A., et al. 2010b, *ApJS*, 187, 460
 Adler, S. L., Bahcall, J. N., Callan, C. G., & Rosenbluth, M. N. 1970, *Phys. Rev. Lett.*, 25, 1061
 Aharonian, F., et al. 2005, *A&A*, 435, L17
 Aliu, E., et al. 2008, *Science*, 322, 1221
 Bai, X., & Spitkovsky, A. 2010, *ApJ*, 715, 1282
 Cheng, K. S., Ho, C., & Ruderman, M. 1986, *ApJ*, 300, 500
 Cohen, R. H., & Treves, A. 1972, *A&A*, 20, 305
 Crawford, F., Manchester, R. N., & Kaspi, V. M. 2001, *AJ*, 122, 2001
 Daugherty, J. K., & Harding, A. K. 1996, *ApJ*, 458, 278
 De Luca, A., Caraveo, P. A., Mereghetti, S., Negroni, M., & Bignami, G. F. 2005, *ApJ*, 623, 1051
 Du, Y., Qiao, G. J., Han, J. L., Lee, K. J., & Xu, R. X. 2010, *MNRAS*, 406, 2671
 Dyks, J., & Rudak, B. 2003, *ApJ*, 598, 1201
 Fierro, J. M. 1995, PhD thesis, Stanford University
 Gaensler, B. M., Arons, J., Kaspi, V. M., Pivovarov, M. J., Kawai, N., & Tamura, K. 2002, *ApJ*, 569, 878
 Gaensler, B. M., Brazier, K. T. S., Manchester, R. N., Johnston, S., & Green, A. J. 1999, *MNRAS*, 305, 724
 Harding, A. K., Baring, M. G., & Gonthier, P. L. 1997, *ApJ*, 476, 246
 Hobbs, G., Lyne, A. G., Kramer, M., Martin, C. E., & Jordan, C. 2004, *MNRAS*, 353, 1311
 Hobbs, G. B., Edwards, R. T., & Manchester, R. N. 2006, *MNRAS*, 369, 655
 Holloway, N. J. 1977, *MNRAS*, 181, 9P
 James, F., & Roos, M. 1975, *Comput. Phys. Commun.*, 10, 343
 Kawai, N., Okayasu, R., Brinkmann, W., Manchester, R., Lyne, A. G., & D’Amico, N. 1991, *ApJ*, 383, L65
 Kuiper, L., Hermsen, W., Krijger, J. M., Bennett, K., Carramiñana, A., Schönfelder, V., Bailes, M., & Manchester, R. N. 1999, *A&A*, 351, 119
 Livingstone, M. A., Kaspi, V. M., Gavriil, F. P., & Manchester, R. N. 2005, *ApJ*, 619, 1046
 Lorimer, D. R., & Kramer, M. 2004, *Handbook of Pulsar Astronomy* (Cambridge: Cambridge Univ. Press)
 Manchester, R. N., Tuohy, I. R., & Damico, N. 1982, *ApJ*, 262, L31
 Mattox, J. R., et al. 1996, *ApJ*, 461, 396
 Matz, S., et al. 1994, *ApJ*, 434, 288
 Melatos, A. 1997, *MNRAS*, 288, 1049
 Mineo, T., Cusumano, G., Maccarone, M. C., Massaglia, S., Massaro, E., & Trussoni, E. 2001, *A&A*, 380, 695
 Muslimov, A. G., & Harding, A. K. 2003, *ApJ*, 588, 430
 Pellizzoni, A., et al. 2009a, *ApJ*, 695, L115
 Pellizzoni, A., et al. 2009b, *ApJ*, 691, 1618
 Pellizzoni, A., et al. 2010, *Science*, 327, 663
 Pittori, C., et al. 2009, *A&A*, 506, 1563
 Romani, R. W. 1996, *ApJ*, 470, 469
 Sako, T., et al. 2000, *ApJ*, 537, 422
 Seward, F. D., & Harnden, F. R., Jr. 1982, *ApJ*, 256, L45
 Tamura, K., Kawai, N., Yoshida, A., & Brinkmann, W. 1996, *PASJ*, 48, L33
 Tavani, M., et al. 2009, *A&A*, 502, 995
 Thompson, D. J. 2004, in *Astrophysics and Space Science Library*, Vol. 304, *Cosmic Gamma-Ray Sources*, ed. K. S. Cheng & G. E. Romero (Dordrecht: Kluwer), 149
 Trussoni, E., Massaglia, S., Caucino, S., Brinkmann, W., & Aschenbach, B. 1996, *A&A*, 306, 581
 Ulmer, M. P., et al. 1993, *ApJ*, 417, 738
 Watters, K. P., Romani, R. W., Weltevrede, P., & Johnston, S. 2009, *ApJ*, 695, 1289
 Weltevrede, P., et al. 2010a, *ApJ*, 708, 1426
 Weltevrede, P., et al. 2010b, *PASA*, 27, 64
 Wilson, R. B., et al. 1993, in *Proc. Los Alamos Workshop, Isolated Pulsars*, ed. K. A. van Riper, R. I. Epstein, & C. Ho (Cambridge: Cambridge Univ. Press), 257
 Zhang, L., & Cheng, K. S. 2000, *A&A*, 363, 575